J. Biochem. 2010;147(2):201–211 doi:10.1093/jb/mvp156

JB THE JOURNAL OF BIOCHEMISTRY

A critical role for highly conserved Glu^{610} residue of oligopeptidase B from *Trypanosoma brucei* in thermal stability

Received July 17, 2009; accepted September 26, 2009; published online October 9, 2009

Nor Ismaliza Mohd Ismail[1], Tsuyoshi Yuasa[1], Keizo Yuasa[1], Yuko Nambu[1,*], Makoto Nisimoto[1], Masaki Goto[1], Hitoshi Matsuki[1], Masahiro Inoue[2], Masami Nagahama[1,†] and Akihiko Tsuji[1,‡]

[1]Department of Biological Science and Technology, University of Tokushima Graduate School, 2-1 Minamijosanjima, Tokushima 770-8506; and [2]Department of Parasitology, Kurume University School of Medicine, 67 Asahi-machi, Kurume, Fukuoka 830-0011, Japan

*Present address: Yuko Nambu, Division of Applied Life Sciences, Graduate School of Agriculture, Kyoto University, Gokasyo, Uji, Kyoto, 611-0011, Japan.
†Present address: Masami Nagahama, Department of Molecular Biochemistry, Meiji Pharmaceutical University, 2-522-1 Noshio, Kiyose, Tokyo 204-8588, Japan.

‡Dr Akihiko Tsuji, Department of Biological Science and Technology, University of Tokushima Graduate School, 2-1 Minamijosanjima, Tokushima 770-8506, Japan. Tel: +81 88 656 7526, Fax: +81 88 655 3861, E-mail: tsuji@bio.tokushima-u.ac.jp

Oligopeptidase B from *Trypanosoma brucei* (Tb OPB) is a virulence factor and therapeutic target in African sleeping sickness. Three glutamic acid residues at positions 607, 609 and 610 of the catalytic domain are highly conserved in the OPB subfamily. In this study, the roles of Glu^{607}, Glu^{609} and Glu^{610} in Tb OPB were investigated by site-directed mutagenesis. A striking effect on k_{cat}/K_m was obtained following mutation of Glu^{607} to glutamine. In contrast, the heat stability of Tb OPB decreased markedly following the single mutation of Glu^{610} to glutamine, although this mutation had significantly less effect on catalytic properties compared with the Glu^{607} mutation. Although no differences were found in the tertiary and secondary structures between wild-type (WT) OPB and the E610Q mutant prior to heat treatment, the E610Q mutant is inactivated more rapidly than WT OPB following heat treatment in a manner correlating with its attendant structural changes. Trypsin digestion showed that the boundary regions between the β-propeller and catalytic domain of the E610Q mutant are unfolded with heat treatment. It is concluded that Glu^{607} is essential for the catalytic activity of Tb OPB and that Glu^{610} plays a critical role in stabilization rather than catalytic activity despite their close proximity.

Keywords: oligopeptidase B/prolyl oligopeptidase/propeller domain/thermal stability/trypanosoma.

Abbreviations: ACTH, adrenocorticotropic hormone; Bz, benzoyl; DTNB, 5,5′-dithiobis (2-nitrobenzoic acid); DSC, differential scanning calorimetry; OPB, oligopeptidase B; POP, prolyl oligopeptidase; MCA, 4-methylcoumaryl 7-amide; Tb, *Trypanosoma brucei*; WT, wild type; Z, carbobenzoxy.

Oligopeptidase B is a member of the prolyl oligopeptidase (POP) family of serine proteases belonging to clan SC, family S9 (*1*) which cleave peptides containing no more than 30 amino acids at the carboxyl side of arginine or lysine. The POP family includes oligopeptidase B (OPB, EC 3.4.21.83), POP (POP, EC 3.4.21.26), dipeptidyl-peptidase IV (DPP IV, EC 3.4.14.5) and acylaminoacyl peptidase (EC 3.4.14.19.1) (*2*, *3*). Recent crystal structure determinations and modelling analysis showed that these enzymes share a similar three-dimensional structure containing a catalytic (peptidase) domain with an α/β hydrolase fold and a β-propeller domain (*4*–*6*). The latter domain of POP comprises a 7-fold repeat of a four-stranded antiparallel β sheet which excludes proteins and large peptides from the active site of the catalytic domain. These members of the POP family have recently attracted much attention as drug targets for neurological diseases (POP) (*6*) and type II diabetes (DPP IV) (*7*), and OPB is a candidate therapeutic target in trypanosomiasis (*8*). OPB is found in Gram-negative bacteria and plants, including ancient eukaryotic unicellular organisms such as *Trypanosoma brucei* and *T. cruzi*, which cause sleeping disease and Chagas' disease, respectively. OPB has been purified from *Escherichia coli* (*9*, *10*), *Salmonella enterica* (*11*), *T. brucei* (*12*, *13*), *T. cruzi* (*14*), *T. evansi* (*15*), *Leishmania amazonensis* (*16*) and wheat (*17*). Targeted deletion of the OPB gene in *T. cruzi* attenuated parasite virulence (*18*). *Trypanosoma* OPB plays an important role in the generation of a signalling ligand for mammalian host cells that is involved in host cell invasion (*18*). OPB from *T. brucei* is released from the dying parasite into the host bloodstream during infection (*19*). OPB remains active since it is not inhibited by plasma protease inhibitors such as α2-macroglobulin or serpins. Anomalous degradation of host peptide hormones such as atrial natriuretic hormones by OPB is involved in the pathogenesis of trypanosomiasis (*19*). In fact, OPB from *T. brucei* has been identified as a target of several trypanocidal drugs such as suramine (*8*). Given that the OPB gene is absent in vertebrates, a highly selective OPB inhibitor which is able to distinguish this peptidase from other human serine peptidases could potentially be employed as a trypanocidal drug. Although preliminary crystallization data of OPB from *T. brucei* was reported (*20*), the high resolution X-ray structure of the active site

and substrate-binding sites of Tb OPB were not delineated. Characterization of the P1 specificity of *Trypanosoma* OPB is essential for the design of selective OPB inhibitors. The three-dimensional structural model of Tb OPB constructed by homology modelling using porcine POP as a template suggests that glutamic acid residues at positions 607 and 609 of the enzyme are key residues that bind to P1 substrate residues (*21*, *22*). Three closely located glutamic acid residues at positions 607, 609 and 610 of *Trypanosoma* OPB are highly conserved in OPB subfamily members but are absent in POP subfamily members. In an effort to investigate the aforementioned suggestions, we evaluated the role of these glutamic acid residues in terms of catalytic properties using site-directed mutagenesis. Our results indicated that Glu^{607} plays a significant role in P1 specificity, although a role for Glu^{609} and Glu^{610} has not been excluded. Furthermore, a novel role of Glu^{610} in the stability of OPB was unexpectedly found in this study.

Materials and methods

Materials

Fluorogenic peptide substrate, ACTH and glucagons were purchased from the Peptide Institute (Osaka, Japan). All other chemicals used were of analytical grade.

Enzyme assay

Oligopeptidase B activity was routinely assayed using carbobenzoxy-Phe-Arg-4-methylcoumaryl 7-amide (*Z*-Phe-Arg-MCA) at 37°C as previously described (*23*). For kinetic analysis, the initial reaction velocity was assayed by recording the changes in fluorescence at 460 nm following excitation at 380 nm at 25°C using a F-3010 fluorescence spectrophotometer (Hitachi, Tokyo) (*24*). Protein was determined by the method of Bradford using BSA as a standard (*25*). The molar concentration of recombinant OPB was calculated by assuming that 84 mg of protein represents 1 μmol of enzyme.

Expression of recombinant OPB

Trypanosoma brucei OPB cDNA was amplified by PCR from the genomic DNA with Pfu polymerase using sense (5′-CACCCAAAC TGAACGTGGTCCAATCGCC-3′) and antisense (5′-CTACTTCC GCGCAGCTGCCGTAC-3′) primers. The PCR product was cloned into the pET/D-TOPO expression vector (Invitrogen, Carlsbad, CA) to create pwOPB. Site-directed mutagenesis was performed using a KOD-Plus-Mutagenesis Kit (TOYOBO, Osaka) with pwOPB as a template. Sequences of sense mutation primers are shown in Table 1. The mutation was confirmed by sequence analysis. For expression, pET/D-TOPO expression vectors for wild-type (WT) and mutants of OPB were transformed into *E. coli* strain BL21. N-terminal poly-histidine-OPBs were expressed by induction of a log-phase culture with 0.1 mM isopropyl-β-D-thiogalactopyranoside (IPTG) for 4 h at 20°C with continuous shaking in the presence of 50 μg/ml ampicillin. Transformants from a 500 ml culture were harvested by centrifugation (9,000 r.p.m., 10 min, 4°C) and then homogenized with 50 ml of 20 mM Tris–HCl buffer (pH 7.5) containing 0.5 M NaCl (buffer A). The homogenate was frozen at −30°C. After 18 h, the homogenate was thawed and sonicated (output, 30 s, 15 cycles) on ice using an Astrason ultrasonic processor XL (Misonix, NY, USA). Following centrifugation at 12,000×*g* for 10 min at 4°C, the supernatant was mixed with 2.0 ml Ni-NTA-agarose (Quiagen, GmbH, Hilden, Germany) and incubated at 4°C with continuous mixing. After 2 h, the gel was packed into a column and washed sequentially with 50 ml of buffer A containing 10 mM, 20 mM and 50 mM imidazole. OPB was eluted with buffer A containing 100 mM imidazole and dialyzed against 50 mM Tris–HCl buffer (pH 7.5) at 4°C. Purified enzyme was concentrated (5–10 mg/ml) by ultrafiltration and then stored in an ice bath. The purity of the enzyme was checked by SDS–PAGE (sodium dodecyl sulfate–polyacrylamide gel electrophoresis) using a 7.5% acrylamide gel (*26*).

Cleavage specificity towards glucagon and ACTH

For the cleavage specificity analysis, 2 nmol of peptide substrates (human glucagon and ACTH) were digested with purified WT, E607Q, E609Q or E610Q (2 nmol/min of Z-Phe-MCA cleaving activity at 37°C) for 16 h. The mixture was then acidified with trifluoroacetic acid and separated by RP-HPLC as previously described (*17*). N-terminal amino acid sequences of the purified peptide fragments were analysed using an automated protein sequencer (Shimadzu PPSQ-10, Kyoto, Japan).

Free SH determination

Free sulphhydryl group was determined using 5,5′-dithiobis (2-nitrobenzoic acid) (DTNB) by Ellman's method (*27*).

Intrinsic fluorescence of OPB

Fluorescence spectra were recorded with a Hitachi F-3010 fluorescence spectrophotometer between 300 and 450 nm using an excitation wavelength of 280 and 295 nm at 20°C. Both excitation and emission slit-widths were set to 5 nm and the scan speed was 60 nm/min.

Differential scanning calorimetry

Calorimetric measurements were performed with a Microcal VP-DSC differential scanning calorimeter (Northampton, MA, USA). Thermal denaturation curves were recorded with a heating scan rate of 0.5°C/min at temperatures between 20 and 70°C. The protein concentration was 1 mg/ml (12 μM) in 50 mM Tris–HCl (pH 7.5).

Table 1. Effect of mutation of Glu^{607}, Glu^{609} and Glu^{610} residues on activity towards various synthetic substrates.

Tb OPB	*Bz*-Arg-MCA[a]			*Z*-Phe-Arg-MCA[a]		
	K_m (μM)	k_{cat} (S^{-1})[b]	k_{cat}/K_m ($\mu M^{-1} S^{-1}$)	K_m (μM)	k_{cat} (S^{-1})[b]	k_{cat}/K_m ($\mu M^{-1} S^{-1}$)
WT	2.68 ± 0.19	13.3 ± 0.24	4.96	3.34 ± 0.20	8.29 ± 0.57	2.48
E607Q	15.0 ± 1.27	1.24 ± 0.05	0.083	11.3 ± 1.64	0.758 ± 0.05	0.067
E609Q	8.07 ± 0.19	15.8 ± 0.20	1.96	5.28 ± 0.59	7.81 ± 0.47	1.48
E610Q	5.86 ± 0.86	15.2 ± 0.67	2.59	5.68 ± 0.33	9.36 ± 0.74	1.65
E607/609Q	7.28 ± 0.23	1.58 ± 0.27	0.217	12.7 ± 2.0	1.64 ± 0.32	0.129
E609/610Q	12.7 ± 1.12	9.53 ± 0.27	0.750	17.3 ± 1.98	11.2 ± 1.98	0.647
E609A	5.25 ± 0.42	5.42 ± 0.70	1.03	10.1 ± 1.27	6.84 ± 0.36	0.677
E609F	6.69 ± 0.70	1.77 ± 0.45	0.265	9.13 ± 0.94	1.46 ± 0.09	0.050
E609R	21.5 ± 2.78	5.37 ± 0.90	0.250	18.4 ± 2.33	1.42 ± 0.22	0.077
E609L	6.37 ± 1.38	5.03 ± 0.25	0.790	9.04 ± 0.74	4.98 ± 0.21	0.551

[a]Unless otherwise stated, the kinetic data and SDs were calculated from at least three separate determinations. [b]Based on a molecular mass of 84 kDa.

Light transmittance measurements

The thermal denaturation temperature ($T_{1/2}$) was also determined by examining the turbidity of a solution containing OPB 0.1 mg/ml in 50 mM Tris–HCl (pH 7.5). The heating scan rate was 0.5°C/min. The transmittance in a quartz cuvette was measured by a U-3900 Spectrophotometer (Hitachi, Tokyo) equipped with a programmable water circulator PCC-7000 (Tokyo Rikakikai, Tokyo) at 560 nm in the same temperature range as the differential scanning calorimetry (DSC). The actual temperature in the sample was measured by a filament thermistor TX-10 (Yokogawa, Tokyo) attached on the cuvette.

Circular dichroism spectra measurements

The circular dichroism (CD) spectra of WT and E610Q OPB (0.5 mg/ml, 6 μM) were measured by scanning in the 200- to 300-nm range with a Jasco J-720 CD spectropolarimeter (Jasco, Tokyo) using a cuvette with a 0.1 cm light path. The solution was maintained at 25°C by circulating water. Spectra were averaged over five scans. The base line of the buffer (50 mM Tris–HCl buffer, pH 7.5) was subtracted for all CD spectra.

Limited proteolysis of OPB by trypsin

WT and E610Q OPB (50 μg) were incubated with trypsin (10 ng) at 40°C for 1 h. The reaction was terminated by the addition of leupeptin and then subjected to SDS–PAGE using a 12% acrylamide gel. The digested fragments separated by SDS–PAGE were electroblotted onto a PVDF membrane (Immobilon, 0.45 mm; Milipore, Bedford, MA, USA) according to the manufacturer's instructions, and N-terminal sequences (five residues) were analysed using an automated protein sequencer (Shimadzu-PPSQ10) to identify the cleavage sites.

Results

Site-directed mutagenesis and expression of WT and mutant OPBs

Glu^{607}, Glu^{609} and Glu^{610} residues are highly conserved in OPB subfamily members (*22*). It is highly likely that these negatively charged OPB residues contribute to the recognition of substrate residues containing basic amino acid side chains such as arginine or lysine (*11*, *21*, *22*). The three-dimensional model of *E. coli* OPB (*4*), Tb OPB (*21*) and a mutagenesis study of Salmonella OPB (*11*) suggested that a pair of glutamic acid residues, Glu^{607} and Glu^{609}, forms the S1 binding site of Tb OPB. The residue equivalent to Glu^{610} is also strictly conserved in OPB subfamily members, suggesting a functional importance associated with this residue. To identify the functional role of Glu^{607}, Glu^{609} and Glu^{610} in Tb OPB, OPB mutants in which the aforementioned glutamic acid residues were replaced with glutamine or other amino acids were purified and characterized. WT *T. brucei* (Tb) OPB and site-mutated variants were expressed in the *E. coli* strain BL21 at 20°C as soluble, catalytically active polyhistidine-tagged enzymes with protein yields between 10 and 20 mg per litre of bacterial culture. The temperature of the culture at the point of induction with IPTG is critical for the production of soluble OPB. At temperatures >30°C, all OPB synthesized was recovered in the precipitate following extraction. All purified recombinant OPBs migrated as single 84 kDa bands on SDS–PAGE under reducing conditions (Fig. 1). Specific activities towards Z-Phe-Arg-MCA at 37°C of WT, E607Q, E609Q, E610Q, E607/609Q and E609/610Q were 27.9, 0.323, 22.1, 20.9, 0.10 and 11.0, respectively. The specific activity decreased markedly following the single mutation of Glu^{607} (1.2% of WT), whereas replacement of Glu^{609} or Glu^{610} with glutamine had no significant effect on specific activity. These results suggested that the negative charge in Glu^{607} is critical for the catalytic activity of Tb OPB.

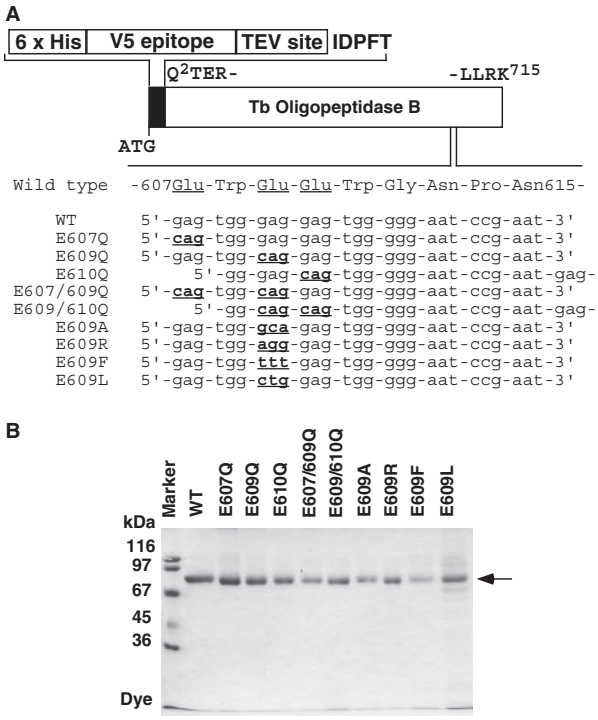

Fig. 1 Schematic structure of recombinant OPB and SDS–PAGE of the purified enzyme. Mutagenic primers used to introduce glutamic acid mutations into Tb OPB are shown. Mutated codons corresponding to amino acid residues at positions 607, 609 and 610 are underlined in bold type. Only sense primers are indicated.

Effect of replacing of Glu^{607}, Glu^{609} and Glu^{610} with glutamine on substrate specificity

In an effort to identify the catalytic role of Glu^{607}, Glu^{609} and Glu^{610} in Tb OPB, the substrate specificity of OPB mutants were investigated using the synthetic substrates *Bz*-Arg-MCA and *Z*-Phe-Arg-MCA. As shown in Table 1, replacement of Glu^{607} with glutamine (E607Q) resulted in significant changes in the hydrolysis of these substrates. This mutation led to a marked reduction in k_{cat} towards *Bz*-Arg-MCA (9.3%) and *Z*-Phe-Arg-MCA (9.1%) in comparison with the WT enzyme. The K_m values for *Bz*-Arg-MCA and *Z*-Phe-Arg-MCA increased 5.1- and 3.4-fold, respectively. In contrast, replacement of Glu^{609} (E609Q) and Glu^{610} (E610Q) with glutamine did not lead to a significant reduction in the k_{cat} values for the substrates tested, unlike the case with the E607Q mutant, whereas increases in the K_m values for *Bz*-Arg-MCA and *Z*-Phe-Arg-MCA were less marked compared with the E609Q mutant. Kinetic constants for the hydrolysis of these substrates by the double mutant E607/609Q were also examined. Compared with the E607Q mutant, additional changes in kinetic constants were not observed. Double mutations involving Glu^{609} and Glu^{610} (E609/610Q) resulted in

slight increases (2- to 3-fold) in the K_m values for these substrates, whereas k_{cat} values did not change significantly. On the other hand, the pair of glutamic acid residues Glu^{576} and Glu^{578} of salmonella OPB (corresponding to Glu^{607} and Glu^{609} of Tb OPB) was reported to define the P1 specificity of OPB (*11*). To confirm the role of Glu^{609} of Tb OPB, kinetic constants of mutants in which Glu^{609} was replaced with alanine, phenylalanine, arginine or leucine were analysed. These mutations (E609A, E609F, E609R and E609L) resulted in a 2- to 3-fold increase in the K_m values for *Bz*-Arg-MCA and *Z*-Phe-Arg-MCA compared with WT OPB. Replacement of Glu^{609} with positively charged arginine (E609R) resulted in greater increases in the K_m values for these substrates compared with E609A, E609F and E609L. Thus, the negative charge in Glu^{607} is critical for the catalytic activity of OPB, although the contribution of Glu^{609} and Glu^{610} in substrate binding has not been excluded.

Hydrolysis of glucagon and ACTH

The cleavage specificity of OPB and mutant enzymes was compared using glucagons and ACTH as model peptides. WT OPB cleaved Lys^{12}–Tyr^{13}, Arg^{17}–Arg^{18} and Arg^{18}–Ala^{19} bonds of glucagons. All mutant OPBs (E607Q, E609Q, E607/609Q and E610Q) also cleaved the aforementioned peptide bonds. Digestion of ACTH by WT OPB generated four peptide fragments (SYSMEHFR, WGK, WGKPVGK and VYP). These results indicated that Arg^{8}–Trp^{9}, Lys^{11}–Pro^{12}, Lys^{15}–Lys^{16}, Arg^{17}–Arg^{18} and Lys^{21}–Val^{22} bonds were preferentially hydrolyzed by WT OPB. Digestion of ACTH by mutant OPB (E607Q, E609Q, E607/609Q and E610Q) generated three fragments (SYSMEHFR, WGKPVGK and VYP). Hydrolysis of the Lys^{11}–Pro^{12} bond by mutant OPB was negligible. The mutant OPBs E609A and E609R cleaved the same peptide bonds of ACTH. These results showed that the mutant OPBs only cleaved the carboxyl side of basic amino acids like the case with WT OPB, although cleavage efficiencies were lower compared with WT OPB.

Increased susceptibility of E610Q mutant to thermal denaturation

Figure 2A shows a comparison of WT and mutant OPB thermal stability at 45°C at pH 7.5. Replacement of Glu^{610} with glutamine (E610Q) resulted in a marked decrease in thermal stability. Following treatment at 45°C for 20 min, the relative activities of WT, E607Q and E609Q were 89, 74 and 84%, respectively, whereas almost all activity of E610Q and E609/610Q was lost. Figure 2B shows the effect of urea on the enzyme activity of WT and mutant OPBs. WT, E607Q and E609Q were resistant to treatment with 3M urea, whereas the E610Q mutant was inactivated to 63% of the control. Reducing reagent such as dithiothreitol had no effect on the inactivation of WT and mutant OPBs by heat and urea treatment.

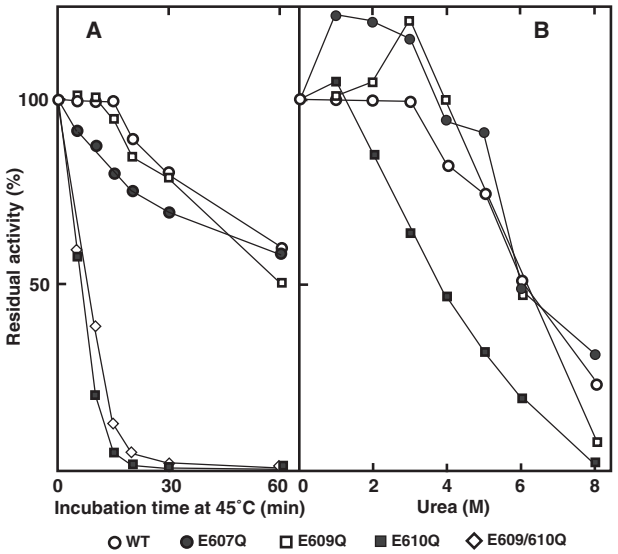

Fig. 2 Effects of heat and urea treatment on the activity of WT and OPB mutants. (A) Tb OPB (0.1 mg/ml in 50 mM Tris–HCl, pH 7.5) treated at 45°C. After 5, 10, 15, 20, 30 or 60 min, the enzyme was immediately cooled in an ice-bath. Enzyme was diluted 50-fold with ice-cold 50 mM Tris–HCl (pH 7.5) and residual activity was assayed. (B) Tb OPB (50 μg/ml) in 50 mM Tris–HCl (pH 7.5) containing 0, 1, 2, 3, 4, 5, 6 or 8 M urea and incubated at 25°C. After 15 min, the enzyme was diluted 10-fold with 50 mM Tris–HCl (pH 7.5) and residual activity was assayed. WT OPB (open circle), E607Q (closed circle), E609Q (open square), E610Q (closed square), E609/610Q (open diamond).

Comparison of thermal stability between WT and E610Q

Light-transmittance measurements and DSC were performed to examine the thermal stability of the E610Q mutant. As shown in Fig. 3A, $T_{1/2}$ of E610Q (49.7°C) was clearly lower than those of WT (53.3°C) and E607Q (55.4°C). The DSC experiments also gave consistent results (Fig. 3B). The E610Q mutant exhibited a markedly lower T_m value (45.2°C) compared with WT OPB, which showed a more complex scanning profile comprising two peaks (T_m values: 53.1 and 55.4°C).

Unfolding of E610Q OPB mutant by heat treatment

Unfolding of the E610Q mutant by heat treatment was analysed by CD and intrinsic protein fluorescence measurements. Figure 4A shows the far-UV CD spectra of WT and E610Q OPB prior to and following heat treatment (42°C, 10 min). This heat treatment did not cause increase of turbidity of a solution containing WT or E610Q. As shown in Fig. 4A-I, the CD spectra of native WT and E610Q OPB prior to heat treatment were almost indistinguishable, indicating that any alteration in the secondary structure caused by the replacement of Glu^{610} with glutamine is less significant. However, the CD spectrum of E610Q following heat treatment changed more significantly than that of WT OPB (Fig. 4A-II, III). These results suggested a reduction in ordered secondary structure of E610Q following heat treatment. Unfolding of the E610Q mutant following heat treatment was also examined by measuring fluorescence changes. Tb OPB contains

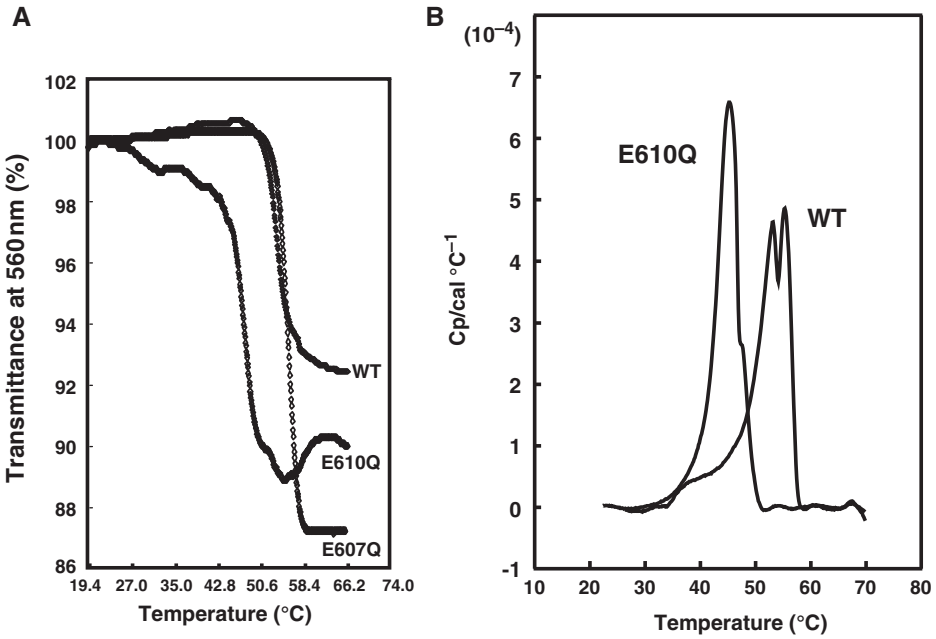

Fig. 3 Analysis of heat denaturation of Tb OPB by transmittance and DSC analyses. (A) Transition temperature, $T_{1/2}$, was measured by examining the turbidity of a solution containing 0.1 mg/ml protein in 50 mM Tris–HCl buffer (pH 7.5) as described under the Experimental procedures section. (B) Denaturation curves recorded with the solution containing 1 mg/ml Tb OPB in 50 mM Tris–HCl (pH 7.5). Experimental conditions were as described in the Experimental procedures section.

11 tryptophan residues (five residues in the β-propeller and six residues in the catalytic domain), with two tryptophan residues (Trp^{608} and Trp^{611}) being present in close proximity to position 610. Therefore, the fluorescence data may reflect changes in the local environments of these tryptophan residues. WT OPB and the E610Q mutant were treated at 40°C for 0, 5, 10 and 20 min. Following centrifugation, fluorescence spectra (emission: 300–450 nm, excitation: 280 and 295 nm) of the supernatants were determined. Proteins did not precipitate following treatment at 40°C for 20 min. As shown in Fig. 4B (left), the fluorescence spectrum of WT OPB did not change significantly following heat treatment. The maximum fluorescence wavelength (333 nm) was constant. In contrast, the fluorescence intensity of the E610Q mutant decreased with increasing heat treatment time and the maximum fluorescence wavelength shifted slightly towards longer wavelength (from 333 to 335 nm). These results indicated that tryptophan residues buried in the interior of the E610Q mutant are exposed to the exterior following heat denaturation.

Effect of heat treatment on SH group titration

Tb OPB contains 10 cysteine residues in the β-propeller domain and four cysteine residues in the catalytic domain. In particular, Tb OPB possesses a unique cysteine residue located near the active site at position 256 (*21*). This residue can be specifically alkylated by reagents such as iodoacetamide, resulting in the inhibition of OPB enzyme activity. Both WT and E610Q enzymes exhibited similar sensitivity to iodoacetamide. The SH groups of WT OPB and

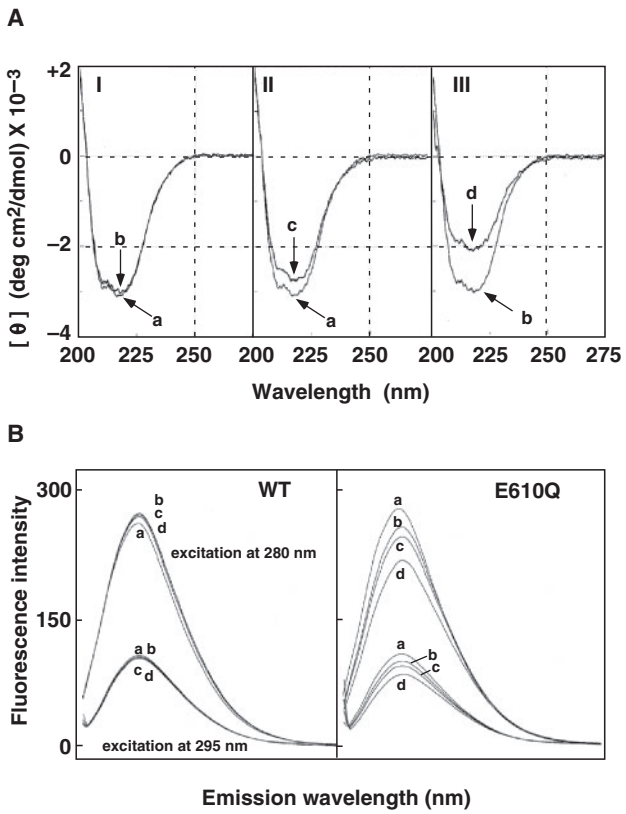

Fig. 4 Effect of heat treatment on CD and fluorescence spectra of WT and E610Q mutant Tb OPB. (A) CD spectra of 5 μM WT and E610Q mutant Tb OPB. Control WT (a), control E610Q (b), WT treated at 40°C for 10 min (c), E610Q treated at 40°C for 10 min (d). (B) Fluorescence spectra of tryptophan residues of WT and E610Q mutant Tb OPB (0.1 mg/ml). Tb OPB treated at 40°C for 0 min (a), 5 min (b), 10 min (c), 20 min (d).

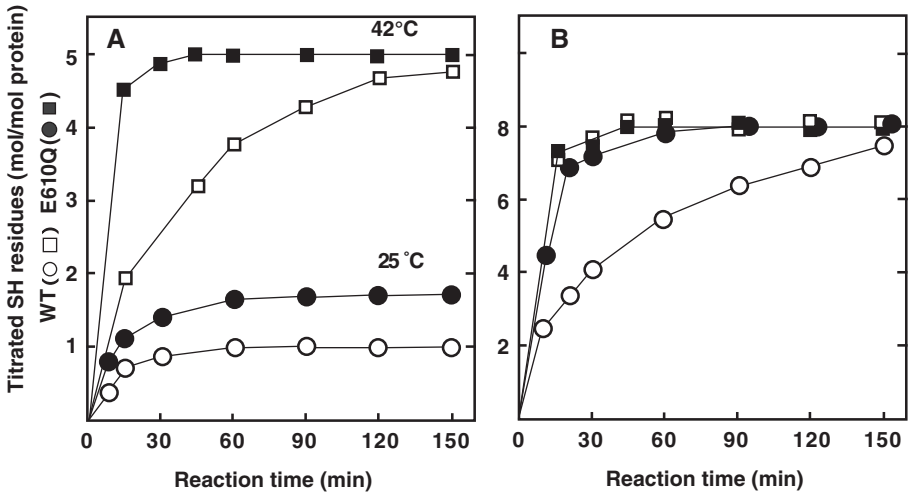

Fig. 5 Progress of the DTNB reaction with sulphydryl groups of WT and E610Q mutant Tb OPB. (A) Enzyme (0.5 mg/ml) was incubated at 25°C or 42°C in 50 mM Tris–HCl (pH 7.5). WT at 25°C (open circle), 42°C (open square); E610Q mutant at 25°C (closed circle), 42°C (closed square). (B) Enzyme (0.5 mg/ml) was incubated at 25°C in the presence of 4 M and 8 M urea in 10 mM Tris–HCl (pH 7.5). WT in 4 M urea (open circle), 8 M urea (open square); E610Q mutant in 4 M urea (closed circle), 8 M urea (closed square). Values are expressed as number of SH groups per 84 kDa Tb OPB.

the E610Q mutant were titrated with DTNB at 25 and 42°C. As shown in Fig. 5A, the number of titrated SH groups per mol of 84 kDa protein at 25°C was 1.04 and 1.72 in the WT and E610Q enzymes, respectively. It is highly likely that the one cysteine residue titrated in WT OPB is Cys^{256}. The E610Q mutant possesses another titrated cysteine residue in addition to Cys^{256}. In reactions at 42°C, approximately five SH groups of the E610Q mutant were titrated after 15 min, whereas only two SH groups were titrated in WT OPB after 15 min and five SH groups were finally titrated after 150 min. These results indicated that the reactivity of three cysteine residues towards DTNB is enhanced following mutation of Glu^{610} to glutamine. The SH groups of urea-denatured WT and E610Q mutant were also titrated (Fig. 5B). The number of total SH groups per 84 kDa protein in 8 M urea-denatured WT and E610Q enzymes was 8.0. These results suggested that Tb OPB had three disulfide bonds. In the presence of 4 M urea, seven SH groups of the E610Q mutant were titrated after 30 min, whereas only four SH groups were titrated in WT OPB after 30 min. These results confirmed that the reactivity of three cysteine residues towards DTNB is enhanced following mutation of Glu^{610} to glutamine.

Increased susceptibility of E610 mutant to trypsin digestion

In an effort to examine differences in the tertiary structure of WT OPB and the E610Q mutant, both proteins (50 µg protein) were incubated with trypsin (10 ng protein) for 60 min at 25°C and 40°C. The extent of proteolysis and apparent molecular mass of the generated fragments were analysed by SDS–PAGE using a 12% acrylamide gel. No fragments were generated from either WT or E610Q following digestion at 25°C (data not shown). Figure 6A shows the digestion patterns of WT and E610Q at 40°C. Several fragments

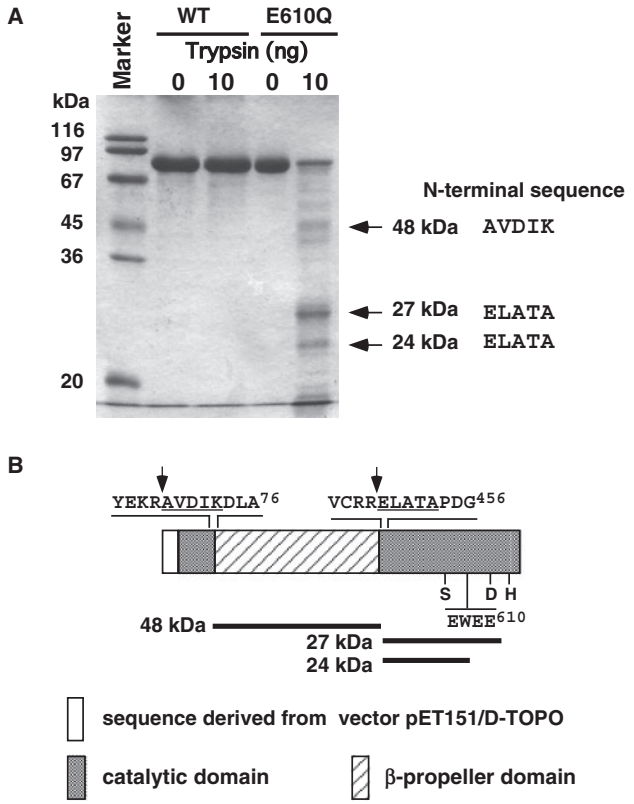

Fig. 6 Trypsin digestion of WT and E610Q mutant Tb OPB at 40°C. (A) SDS–PAGE (12% acrylamide gel) of WT and E610Q mutant Tb OPB digested with trypsin at 40°C for 1 h and N-terminal sequence of 48, 27 and 24 kDa fragments identified by Edman degradation. (B) Schematic view of the structure of Tb OPB, proteolytic digestion fragments and corresponding cleavage sites. Active site residues (Ser^{563}, Asp^{648} and His^{683}) are also shown.

(48, 27 and 24 kDa) were generated from the E610Q mutant, while WT OPB remained impervious to digestion even at 40°C. The cleavage sites within the E610Q mutant were identified by amino acid

sequence analysis. OPB possesses two domain structures consisting of a predominantly C-terminal catalytic domain (residues 1–72 and 428–710 in POP) and an N-terminal β-propeller domain (73–427 in POP), as shown in Fig. 6B. The E610 mutant was cleaved by trypsin at Arg^{68}–Ala^{69} and Arg^{448}–Glu^{449} bonds. Both cleavage sites are located at the boundary region between the β-propeller and catalytic domains. These results indicated that the boundary region between the β-propeller and catalytic domains is unfolded and susceptible to cleavage by trypsin.

Effect of salt on the thermal stability of E610Q mutant

The addition of salt stabilizes *E. coli* OPB against irreversible thermal denaturation (*28*). The effect of high concentrations (1 and 2 M) of NaCl and $(NH_4)_2SO_4$ on the thermal inactivation of E610Q was examined (Fig. 7). Both control WT OPB and E610Q mutant enzyme activities were slightly inhibited following treatment with high concentrations of $(NH_4)_2SO_4$. On the other hand, inclusion of salt led to marked stabilization of the E610Q mutant against thermal inactivation. However, following inactivation of the E610Q mutant by heat treatment, the enzyme was not reactivated by the addition of 2 M NaCl or $(NH_4)_2SO_4$. The effect of salt on the structure of OPB was examined by fluorescence measurements and gel filtration (Fig. 8). Fluorescence spectra of WT and E610Q mutant tryptophanyl residues following heat treatment (45°C, 10 min) in the absence or presence of 2 M NaCl were measured. In these experiments, the relative enzyme activity of WT OPB treated with 2 M NaCl at 0°C for 10 min was 102% of the control. The activities of WT OPB following heat treatment in the absence or presence of 2 M NaCl were 81.3 and 72% of the control, respectively. The activity of E610Q treated with 2 M NaCl at 0°C was 96.5% of the control. The activities of the E610Q mutant following heat treatment in the absence or presence of NaCl were 17.2 and 51.4% of the control. Heat treatment of WT OPB resulted in slight decreases in fluorescence intensity and a shift in the maximum fluorescence wavelength toward longer wavelength from 333 nm to 335 nm (Fig. 8A, upper). However, the effect of 2 M NaCl on the spectra was insignificant. In contrast, the marked decreases in fluorescence intensity and shift in the maximum fluorescence wavelength from 333 nm to 337 nm observed for the E610Q mutant following heat treatment was partially attenuated by NaCl (Fig. 8A, lower). The OPBs employed for the fluorescence measurements were subjected to Superdex 200 PC3.2/30 gel filtration. As shown in Fig. 8B-I,-II, the molecular mass of control WT OPB and the E610Q mutant was estimated to be 160 kDa, suggesting that Tb OPB is a dimer like OPB from *T. cruzi* (*29*). The E610Q mutant following heat treatment in the absence of NaCl was eluted as two peaks (Fig. 8B-III). The first peak, which lacked enzyme activity, was eluted as high-molecular weight form in the void volume. The second peak, having enzyme activity, was eluted as a 160 kDa protein as was the case with native OPB. The E610Q mutant following heat treatment in the presence of NaCl was eluted as a single peak, and an inactive high molecular weight form was not detected. It is highly likely that high concentrations of salt guard the E610Q mutant from aggregation following heat treatment.

Discussion

Strict conservation of glutamic acid residues Glu^{607}, Glu^{609} and Glu^{610} of the catalytic domain of OPB subfamily members indicates that these residues play an important structural or functional role. By employing homology modelling based on a high-resolution X-ray structure of porcine POP as a template, a three-dimensional model structure was constructed for OPB from *E. coli* (*4*) and *L. amazonensis* (*16*). These data suggested that the Glu^{607} and Glu^{609} pair

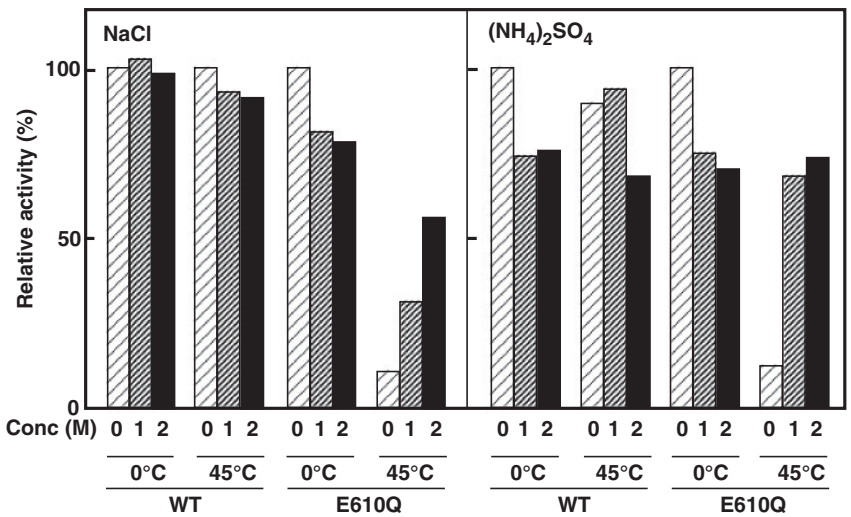

Fig. 7 Effect of high concentrations of salt on thermal inactivation of the E610Q mutant. WT and E610Q mutant Tb OPB (0.1 mg/ml in 50 mM Tris–HCl, pH 7.5) were treated at 45°C for 10 min. Following a 40-fold dilution with 50 mM Tris–HCl (pH 7.5), the residual activity was assayed using *Z*-Phe-Arg-MCA. As a control, these enzymes were treated at 0°C for 10 min.

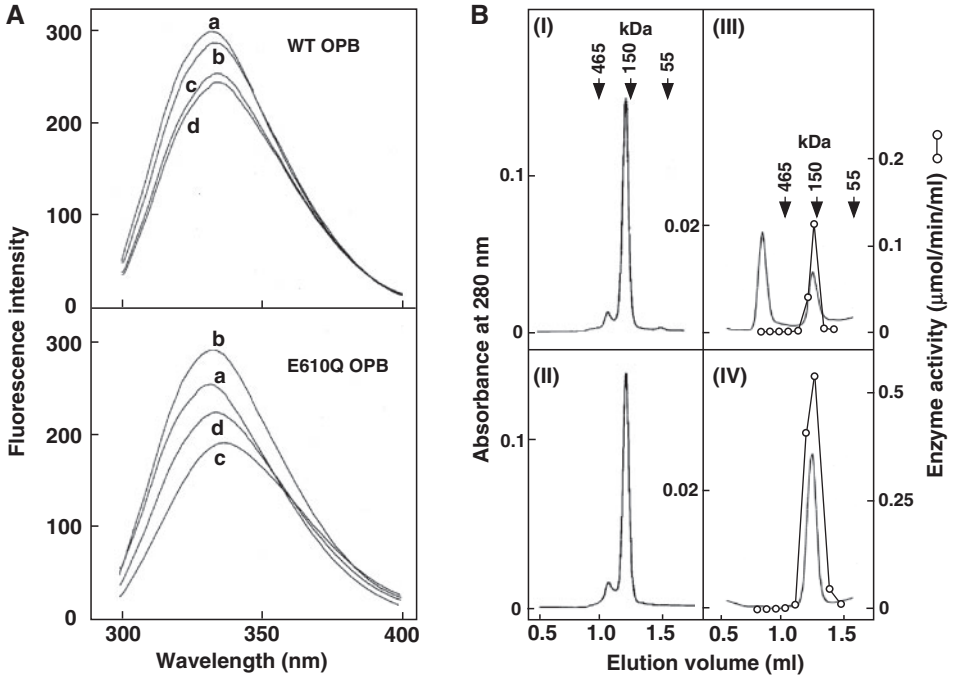

Fig. 8 Effect of NaCl on thermal denaturation of the E610Q mutant. (A) Fluorescence spectra (excitation at 280 nm) of WT and E610Q mutant Tb OPB (0.1 mg/ml) treated at 45°C for 10 min in the absence or presence of 2 M NaCl. (a) control: treated at 0°C, (b) treated at 0°C in the presence of 2 M NaCl, (c) treated at 45°C, (d) treated at 45°C in the presence of 2 M NaCl. (B) Gel filtration of WT and E610Q mutant Tb OPB treated at 45°C for 10 min. Control WT (I) and E610Q mutant (II) Tb OPB (50 μg protein), E610Q (5 μg) treated at 45°C for 10 min in the absence (III) or presence (IV) of 2 M NaCl, was applied to a Superdex 200 PC 3.2/30 (GE Healthcare, Uppsala, Sweden) column equilibrated with 50 mM Tris–HCl (pH 7.5) containing 0.1 M NaCl and then eluted with the same buffer at a flow rate of 40 μl/min.

of residues represents the binding site of P1 substrate basic amino acid residues. Morty *et al.* (*11*) investigated the role of nine acidic residues that are conserved in OPB, but absent in POP, in terms of the catalytic properties of the enzyme. Glu^{576} and Glu^{578} (corresponding to Glu^{607} and Glu^{609} of Tb OPB) of OPB from *Salmonella enterica* were mutated to Ala and the effect on catalytic activity towards carbobenzyloxy-Arg-MCA was analysed. Mutation of Glu^{576} caused a 7.6-fold increase in the K_m and a 4.5-fold decrease in the k_{cat} compared with WT OPB. Replacement of Glu^{578} with alanine resulted in a 3.7-fold increase in K_m and a 2.3-fold decrease in k_{cat}. Replacement of both Glu^{576} and Glu^{578} with alanine resulted in complete loss of enzyme activity. The effect of replacing Glu^{579}, corresponding to Glu^{610} in Tb OPB, with alanine on catalytic activity was not reported. They concluded that Glu^{576} and Glu^{578} (corresponding to Glu^{607} and Glu^{609} in Tb OPB) are critically involved in the interaction of OPB with the basic amino acid of the P1 site of the substrate and speculated that the side chains of Glu^{576} and Glu^{578} form a carboxyl dyad that electrostatically binds the basic side chains of arginine and lysine residues in the substrate. In this article, we prepared histidine-tagged WT enzyme, E607Q, E609Q, E607/609Q, E610Q and E609/610Q mutants of Tb OPB and compared their respective catalytic properties (Table 1). The kinetic properties of recombinant Tb OPB possessing a histidine tag at the N-terminus were reported to be identical to the properties of native enzyme purified from trypanosomes (*13*). In comparison with Salmonella OPB, the k_{cat} of Tb OPB was markedly lower following the single mutation of Glu^{607} (corresponding to Glu^{576} in Salmonella OPB) to glutamine. The k_{cat} values for *Bz*-Arg-MCA and *Z*-Phe-Arg-MCA were 9.3 and 9.1%, respectively, that of the k_{cat} of WT Tb OPB. The double mutation involving Glu^{607} and Glu^{609} in Tb OPB had no additional effect on k_{cat}. The k_{cat} values of the Tb OPB E609Q mutant for the substrates tested were almost identical to the values of WT Tb OPB. The effect of Glu^{609} mutation on the K_m for *Bz*-Arg-MCA and *Z*-Phe-Arg-MCA was less marked compared with the effect of Glu^{607} mutation. Replacement of Glu^{609} with alanine had a greater effect on k_{cat}/K_m than replacement with glutamine. E609Q displayed an approximate two-fold higher k_{cat}/K_m value than E609A, suggesting that the hydrophobicity of the alanine side chain has a negative effect on the catalytic activity of OPB. Morty *et al.* (*11*) investigated the role of Glu^{578} in *Salmonella* OPB following mutation to alanine, hence its catalytic role might be overestimated. Tb OPB, E609F, E609R and E609L all had lower k_{cat}/K_m values compared with E609Q. This difference is likely to result from steric hindrance. Thus, our data indicated that residue Glu^{607} essentially defines the P1 specificity of Tb OPB. However, cleavage specificity of Tb OPB towards model peptides remained unchanged following mutation of Glu^{607} and Glu^{609}. These mutant enzymes specifically cleaved the C-terminal side of basic amino acid residues in glucagons and ACTH, as was the case with WT OPB. These results

suggested that other acidic residues might contribute towards P1 specificity.

On the other hand, the thermal stability of Tb OPB decreased markedly following the single mutation of Glu^{610} to glutamine (Fig. 2), although significant differences in the protein structure between WT and the E610Q mutant prior to heat treatment were not detected. The E610Q mutant was also more labile against urea denaturation compared with WT or other mutants. These results are consistent with those results obtained for the transmittance and DSC measurements (Fig. 3), fluorescence spectra and far-UV CD (Fig. 4) analyses. DSC measurement showed that the T_m of the E610Q mutant (42.2°C) is ~10°C lower than that of WT Tb OPB. The DSC curves of WT OPB exhibited two very close peaks (T_m: 53.8 and 55.4°C). Both peaks shifted to a lower temperature region by following mutation of Glu^{610} to glutamine. Juhász *et al*. (*30*) compared the thermal stability of native POP and a recombinant β-propeller domain by DSC measurement (*30*). Although native POP also exhibited two peaks on the DSC curves (T_m values: 44.6°C and 52.8°C), as seen the case of Tb OPB, their profiles differed. In contrast, the recombinant β-propeller domain of POP exhibited a higher T_m value (59.8°C) compared with native POP. They concluded that an unclosed propeller is more heat-stable than the whole POP molecule, and that the attached catalytic domain reduces the stability of the β-propeller domain. Our DSC analysis of Tb OPB indicated that the single mutation of Glu^{610} in the catalytic domain reduces not only the thermal stability of catalytic domains but also that of the β-propeller domain. Furthermore, heat treatment increased susceptibility of the E610Q mutant to trypsin digestion, although that of WT OPB remained unaffected (Fig. 6). The catalytic domain of OPB comprises short N-terminal and long C-terminal fragments, and residues between these two portions constitute the β-propeller domain. The C-terminal sides of Arg^{68} and Arg^{448} in the boundary regions between these domains of the E610Q mutant were cleaved with trypsin at 40°C, although no cleavage occurred at 25°C. One additional cysteine residue was titrated in the E610Q mutant at 25°C. It is highly likely that this additional cysteine residue is Cys^{446}, located near the cleavage site (Arg^{448}). These results indicate that the boundary regions between the β-propeller and catalytic domains of the E610Q mutant unfold easily following heat treatment.

Porcine POP possesses an aspartic acid residue at position 598, corresponding to Glu^{610} in Tb OPB, and this aspartic acid residue is highly conserved in POP subfamily members (*31*). These data suggested that Asp^{598} in POP plays a similar structural role to Glu^{610} in OPB. The three-dimensional structure of porcine POP shows that the side chain of Asp^{598} binds to Phe^{476} and His^{515} residues by hydrogen bonds (*3*). Phe^{476} and His^{515} residues are located at the boundary region between the β-propeller and catalytic domains of POP. Tyr^{485} and Tyr^{523} residues in Tb OPB correspond to Phe^{476} and His^{515} residues, respectively, in POP. Tyr^{485} and Tyr^{523} residues are also highly conserved in OPB subfamily members. Although replacement of Glu with Gln would still allow for the formation of hydrogen bonds, these bonds would probably be weaker. Trypsin digestion of the E610Q mutant at 40°C indicated that the region around Arg^{448} becomes unfolded following heat treatment. Mutation of Glu^{610} to Gln might result in the loss or formation of weaker hydrogen bonds between Glu^{610} and Tyr^{485} or Tyr^{523}.

The Tb OPB E610Q mutant was also guarded against heat inactivation by high concentrations of salt (Fig. 7), as was the case with *E. coli* OPB (*28*). The addition of salt following heat treatment had no effect on the activity. $(NH_4)_2SO_4$ was more effective at guarding against heat inactivation compared with NaCl. Fluorescence spectra and gel filtration analyses confirmed the effect of high concentrations of salt on thermal denaturation. With gel filtration, both the WT enzyme and E610Q mutant eluted as dimers, as reported by Burleigh *et al* (*29*). Heat treatment of the E610Q mutant resulted in the formation of an inactive high-molecular-weight form, and monomeric OPB was not generated. Formation of inactive enzyme following heat treatment was blocked by the presence of 2 M NaCl. The ability of high concentrations of salt to guard the E610Q mutant against thermal inactivation is not directly explained by a loss of hydrogen bonds. Although formation of less than ideal hydrogen bonds in the E610Q mutant might be attenuated by high concentrations of salt, it is likely that electrostatic interactions play a key role in the heat-induced irreversible denaturation of the E610Q mutant. A determination of the precise position and nature of the Glu^{610} residue in Tb OPB is required to further our understanding of the role played by this residue in protein folding.

One characteristic structural feature of POP family members is the lack of a propeptide. POP family enzymes are synthesized directly as active enzymes, whereas proteases are generally synthesized as inactive precursors (zymogens). Propeptides possess dual roles as intramolecular chaperones and protease inhibitors. Propeptides play an essential role in the correct folding of protease molecules. Following removal of the propeptide, the protease is converted to a mature active form. POP family enzymes selectively cleave oligopeptides not greater that ~30 amino acid residues in length (2). Therefore, the role of the β-propeller domain of POP family members has been investigated to date from the viewpoint of how substrate size is selected or how substrates acquire access to the active site. Recently, Guedes *et al*. (*16*) predicted the presence of a salt bridge between the β-propeller and catalytic domains in OPB from *L. amzonensis*, comprising Asp^{134} of the β-propeller (corresponding to Glu^{127} of Tb OPB) and Arg^{664} of the catalytic domain (corresponding to Arg^{650} of Tb OPB), using homology modelling with porcine POP. Furthermore, Yang *et al*. (*32*) reported that Glu^{88} in the β-propeller domain of acylpeptide hydrolase, a member of the POP family, forms a salt bridge with Arg^{526} in the catalytic domain, and that this salt bridge helps to impart heat stability. These results indicated that two domains of POP family members mutually interact

to generate a stable structure. It is important to determine precisely how the β-propeller domain interacts with the catalytic domain to generate an active and stable structure during biosynthesis.

Acknowledgements

We would like to thank Drs Kazuko Yorita (Institute for Enzyme Research, The University of Tokushima), Yoshitaka Nakajima and Tadashi Yoshimoto (Graduate School of Biomedical Science, Nagasaki University) for valuable discussions. We also thank Ms. Yuka Sasaki for the determination of amino acid sequences.

Conflict of interest
None declared.

References

1. Barrett, A.J. and Rawlings, N.D. (1995) Families and clans of serine peptidases. *Arch. Biochem. Biophys.* **318**, 247–250
2. Polgár, L. (2002) The prolyl oligopeptidase family. *Cell. Mol. Life Sci.* **59**, 349–362
3. Fülöp.V., Böcskei, Z., and Polgár, L. (1998) Prolyl oligopeptidase: a usual beta-propeller domain regulates proteolysis. *Cell* **94**, 161–170
4. Gérczei, T., Kesurü, G.M., and Náray-Szabó, G. (2000) Construction of a 3D model of oligopeptidase B, a potential processing enzyme in prokaryotes. *J. Mol. Graph. Model* **18**, 7–17
5. Hiramatsu, H., Kyono, K., Higashiyama, Y., Fukushima, C., Shima, H., Sugiyama, S., Inaka, K., Yamamoto, A., and Shimizu, R. (2003) The structure and function of human dipeptidyl peptidase IV, possessing a unique eight-bladed β-propeller fold. *Biochem. Biophys. Res. Commun.* **302**, 849–854
6. Maes, M., Goossens, F., Scharpé, S., Meltzer, H.Y., D'Hondt, P., and Cosyns, P. (1994) Lower serum prolyl endopeptidase enzyme activity in major depression: further evidence that peptidases play a role in the pathophysiology of depression. *Biol. Psychiatry* **35**, 545–552
7. Wiedeman, P.E. and Trevillyan, J.M. (2003) Dipeptidyl peptidase IV inhibitors for the treatment of impaired glucose tolerance and type 2 diabetes. *Curr. Opin. Investig. Drugs* **4**, 412–420
8. Morty, R.E., Troeberg, L., Powers, J.C., Ono, S., Lonsdale-Eccles, J.D., and Coetzer, T.H.T. (1998) A trypanosome oligopeptidase as a target for the trypanocidal agents pentamidine, diminazene and suramin. *FEBS Lett.* **433**, 251–256
9. Pacaud, M. and Richard, C. (1975) Protease II from *Escherichia coli*. Purification and characterization. *J. Biol. Chem.* **250**, 7771–7779
10. Kanatani, A., Masuda, T., Shimoda, T., Misoka, F., Lin, X. S., Yoshimoto, T., and Tsuru, D. (1991) Protease II from *Escherichia coli*: sequencing and expression of the enzyme gene and characterization of the expressed enzyme. *J. Biochem.* **110**, 315–320
11. Morty, R.E., Fülöp.V., and Andrews, N.W. (2002) Substrate recognition properties of oligopeptidase B from Salmonella enterica serovar Typhimurium. *J. Bacteriol.* **184**, 3329–3337
12. Troeberg, L., Pike, R.N., Morty, R.E., Berry, R.K., Coetzer, T.H.T., and Lonsdale-Eccles, J.D. (1996) Proteases from Trypanosoma brucei brucei. Purification, characterization and interactions with host regulatory molecules. *Eur. J. Biochem.* **238**, 728–736
13. Morty, R.E., Lonsdale-Eccles, J.D., Morehead, J., Caler, E. V., Mentele, R., Auerswald, E.A., Coetzer, T.H.T., Andrews, N.W., and Burleigh, B.A. (1999) Oligopeptidase B from Trypanosoma brucei, a new member of an emerging subgroup of serine oligopeptidases. *J. Biol. Chem.* **274**, 26149–26156
14. Santana, J.M., Grellier, P., Rodier, M.H., Schrevel, J., and Teixeira, A. (1992) Purification and characterization of a new 120 kDa alkaline proteinase of *Trypanosoma cruzi*. *Biochem. Biophys. Res. Commun.* **187**, 1466–1473
15. Morty, R.E., Pellé, R., Vadász.I, Uzcanga, G.L., Seeger, W., and Bubis, J. (2005) Oligopeptidase B from *Trypanosoma evansi*. A parasite peptidase that inactivates atrial natriuretic factor in the bloodstream of infected hosts. *J. Biol. Chem.* **280**, 10925–10937
16. Guedes, H.L.M., Carneiro, M.P.D., Gomes, D.C.O., Rossi-Bergmanmn, B., and Simone, S.G. (2007) Oligopeptidase B from Leishmania amazonensis: molecular cloning, gene expression analysis and molecular model. *Parasitol. Res.* **101**, 853–863
17. Tsuji, A., Yuasa, K., and Matsuda, Y. (2004) Identification of oligopeptidase B in higher plants. Purification and characterization of oligopeptidase B from quiescent wheat embryo, Triticum aestivum. *J. Biochem.* **136**, 673–681
18. Burleigh, B.A. and Woolsey, A.M. (2002) Cell signalling and *Trypanosoma cruzi* invasion. *Cell. Microbiol.* **4**, 701–711
19. Morty, R.E., Lonsdale-Eccles, J.D., Mentele, R., Auerswald, E.A., and Coetzer, T.H.T. (2001) Trypanosome-derived oligopeptidase B is released into the plasma of infected rodents, where it persists and retains full catalytic activity. *Infect. Immun.* **69**, 2757–2761
20. Rea, D., Hazell, C., Andrews, N.W., Morty, R.E., and Fülöp.V. (2006) Expression, purification and preliminary crystallographic analysis of oligopeptidase B from *Trypanosoma brucei*. *Acta Crystallogr. Sect. F: Struct. Biol. Cryst. Commun.* **62**, 808–810
21. Morty, R.E., Shih, A.Y., Fülöp.V., and Andrews, N.W. (2005) Identification of the reactive cysteine residues in oligopeptidase B from Trypanosoma brucei. *FEBS Lett.* **579**, 2191–2196
22. Coetzer, T.H.T., Goldring, J.P.D., and Huson, L.E.J. (2008) Oligopeptidase B: a processing peptidase involved in pathogenesis. *Biochimie* **90**, 336–344
23. Tsuji, A. and Kurachi, K. (1989) Isolation and characterization of a novel large protease accumulated in mammalian cells in the presence of inhibitors. *J. Biol. Chem.* **264**, 16093–16099
24. Tsuji, A., Yoshimoto, T., Yuasa, K., and Matsuda, Y. (2006) Protamine: a unique and potent inhibitor of oligopeptidase B. *J. Pep. Sci.* **12**, 65–71
25. Bradford, M.M. (1976) A rapid and sensitive method for the quantitation of microgram quantities of protein utilizing the principle of protein-dye binding. *Anal. Biochem.* **72**, 248–254
26. Laemmli, U.K. (1970) Cleavage of structure proteins during the assembly of the head of bacteriophage T4. *Nature* **227**, 680–685
27. Ellman, G.L. (1959) Tissue sulfhydryl groups. *Arch. Biochem. Biophys.* **82**, 70–77
28. Polgár, L. and Felföldi, F. (1998) Oligopeptidase B: cloning and probing stability under nonequilibrium conditions. *Proteins* **30**, 424–434
29. Burleigh, B.A., Caler, E. V., Webster, P., and Andrews, N.W. (1997) A cytosolic serine endopeptidase from *Trypanosoma cruzi* is required for the generation of

Ca^{2+} signaling in mammalian cells. *J. Cell. Biol.* **136**, 609–620
30. Juhász, T., Szeltner, Z., Fülöp.V., and Polgár, L. (2005) Unclosed beta-propellers display stable structures: implications for substrate access to the active site of prolyl oligopeptidase. *J. Mol. Biol.* **346**, 907–917
31. Bastos, M. I., Grellier, P., Martins, N.F., Cadavid-Restrepo, G., de Souza-Ault, M.R., Augustyns, K., Teixeira, A.R., Schrével, J., Maigret, B., da Silveira, J.F., and Santana, J.M. (2005) Molecular, functional and structural properties of the prolyl oligopeptidase of *Trypanosoma cruzi* (POP Tc80), which is required for parasite entry into mammalian cells. *Biochem. J.* **388**, 29–38
32. Yang, G., Bai, A., Gao, L., Zhang, Z., Zheng, B., and Feng, Y. (2009) Glu88 in the non-catalytic domain of acylpeptide hydrolase plays dual roles: charge neutralization for enzymatic activity and formation of salt bridge for thermodynamic stability. *Biochim. Biophys. Acta* **1794**, 94–102